

Magnitude of vibration triggering component determines safety of structures

S. K. Mandal^{1*}, N. K. Bhagat¹, M. M. Singh¹

1. CSIR-Central Institute of Mining & Fuel Research, Dhanbad, India

Received 6 March 2013; received in revised form 20 May 2014; accepted 2 June 2014

**Corresponding author: skm.cimfr@gmail.com (S. K. Mandal).*

Abstract

Transmission of blast waves is a complex phenomenon and the characteristics vary with blast design parameters and geo-technical properties of medium. Frequency of vibration and triggering component for structural excitation generally quantifies safe vibration magnitude. At closer distance or higher elevations than the blast locations, vertical or transverse component will be the first arrival to trigger the sensor for monitoring and at far off distances longitudinal component triggers the sensor to monitor. Similarly, for shorter depth of blastholes and wider blast geometries, vertical or transverse component triggers the sensor to monitor even for longer distances of measurement. Analyzing the cause of such occurrence, the paper firstly puts forward a mathematical model to illustrate the same. Thereafter, considering single-degree of freedom for dynamic analysis of structures, the paper communicates that incident particle velocity exiting a structure to vibrate should be considered to limit vibration magnitude for safety of structures.

Keywords: *Blasting, Magnitude of Vibration, Wave, Structural Analyses.*

1. Introduction

Blasting operations and probable damages to structures is always a point of confrontation between mine management and local inhabitants. There has been a dearth of published information and research activities carried out related to blast designs and documented damage to structures. Considering type of construction, frequency of vibration and distance of structures to blasts, various countries have stipulated legislation to limit magnitude of peak particle velocity [1-3]. Various authors, on contrary, have also commented that the stipulated safe limits are based on human response and not on actual structural damage [4, 5]. Magnitude of maximum particle velocity generally influences the characteristics of peak particle velocity vis-à-vis response of structure towards vibration and therefore, particle velocity should be considered to ascertain limit of vibration magnitude for safety of structures. Furthermore, soil-structure

interaction and dimensions of structure being important parameters to ascertain response of structure towards vibration, safe limit of vibration should be evaluated by monitoring vibration on structures and not on ground [6-8]. Depending upon structure location to source of vibration, vibration monitored on structures may show some anomaly *i.e.*, for surface blasting and surface measurement, attenuation in vibration magnitude may be observed with an increase in height of measurement. Similarly, for underground blasting and monitoring of vibration at different heights on a structure located on surface, amplification in vibration magnitude may be observed with an increase in height of measurement on structures [9, 10]. So, considering wave transmission characteristics in the direction of concern, the paper firstly discusses about the plausible causes of such occurrence and thereafter attempted to develop a mathematical

model to understand the cause of such occurrences. Lastly, considering single-degree of freedom for dynamic analysis of structures, the paper communicates that incident particle velocity exiting the structure to vibrate determines safe vibration limits.

2. Wave behaviour

Propagation characteristics of blast waves vary with rock mass properties and angle of incident on joint plane. Quantum of energy absorbed, reflected and refracted during transmission depend upon thickness of each stratum, smoothness of joint plane and characteristics of filling material within joints [11-15]. At any point of incidence, the angle of incident is always equal to angle of reflection and the angle of refraction varies with the ratio of product of density and P-wave velocity of two mediums (Figure 1). Multiple reflection of stress waves within joints sometimes deteriorate the cohesive characteristics of filling material and result into attenuation in velocity of blast waves generated from consecutive holes fired with some delay in the same round. Transmission of blast-induced stress wave progresses with depleting amplitude and is a function of Poisson's ratio, μ , friction angle, ϕ , and orientation of structural plane, β . Magnitude of

transmitted and reflected wave can be determined with the help of transmission coefficient (A_s) and reflection coefficient (A_z), given in Equations 1 and 2 respectively. Similarly, reduction in pressure of transmitted wave can be determined with the help of Equation 3 [16, 17]. The tri-axial sensor on getting triggered starts monitoring vibration in three orthogonal directions viz., longitudinal, vertical and transverse. The primary or compression wave *i.e.*, body wave is fastest amongst all and are high frequency vibration with least probable damaging characteristics to structures. These waves do not change shape and volume of medium through which it travels. The transverse or shear waves moving perpendicular to the direction of wave propagation changes shape, but, not volume of the material through which it propagates. Rayleigh waves, carrying about 70–80% of the total energy, also known as surface waves, are slowest and characterized by the elliptical particle orbit in the direction contrary to the propagation direction of wave. Surface waves being low frequency vibration possesses more energy and is detrimental to structural stability. S-wave velocity, typically around 60% of primary or P-wave velocity, can be determined with the help of Equation 4.

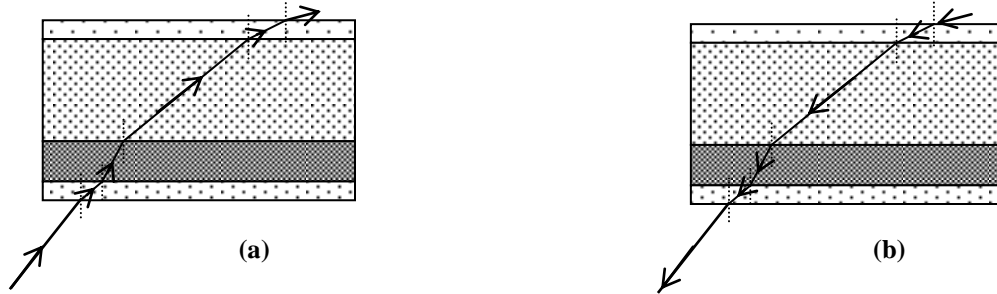


Figure 1. Blast wave transmission characteristics in different mediums

$$A_s = \frac{\text{ctg}(2\beta) + \tan\phi}{\text{ctg}(2\beta) + (\sin(2\alpha)/\cos(2\beta))\eta^2} \quad (1)$$

$$A_z = \frac{(\sin(\alpha)/\cos(2\beta))\eta^2 - \tan(\phi)}{\cos(2\beta) + [\text{Sin}(2\alpha)/\text{Cos}(2\beta)]\eta^2} \quad (2)$$

$$P_j = \frac{2\rho_j c_j}{\rho_j c_j + \rho_r c_r} P_r \quad (3)$$

$$V_p = \sqrt{\frac{k + \frac{4\nu}{3}}{\rho}} \text{ and } V_s = \sqrt{\frac{\nu}{\rho}} \quad (4)$$

Where,

k = Bulk Modulus;

ν = Shear modulus;

ρ = Mass density;

E = Young's modulus; and

μ = Poisson ratio of rock.

Properties of rockmass, characteristics of stratification viz., number and thickness of each

stratum, and type of filling material within joints along the direction of wave propagation determines the triggering component viz., vertical/transverse or longitudinal. For any opencast blast, triggering component depends upon sensor location with respect to blast (horizontal distance and vertical elevation) and the blast geometry implemented at site (Figure 2a), [18]. Similar will be the occurrence during vibration monitoring on surface for the blasts conducted in underground mines (Figure 2b). Blast waves generated from underground blasts generally trigger sensor by either vertical or transverse component. However, when the sensor is located at greater horizontal distances in comparison to vertical cover or in presence of workings or caved or stowed out area between the blasting place and sensor location, longitudinal component will trigger the sensor to monitor. Presence of voids or workings above the blast location causes attenuation in body wave velocity and allows a combination of body and surface wave viz., longitudinal component to trigger sensor for monitoring. Velocity of P-wave for different rock types, determined in laboratory, is shown in Table 1. However, presence of joints results into reduction in P-wave velocity with increase in distance of monitoring, possibly due to

absorption of energy during collision of particles for wave propagation.

3. Vector analyses of vibration components

Detonation of chemical energy stored within explosive are transformed into different forms of kinetic and potential energy and transmitted to surroundings. The unacceptable forms of kinetic energy viz., air concussion and vibration, transmitted through gaseous and solid or liquid medium cause nuisance and damage to surrounding structures located around blast site. Velocity and duration of oscillating particles within elastic zone depends upon borehole pressure i.e., time lapsed between detonation of explosive and release of entrapped gaseous energy through the cracks generated during blasting. So, the kinetic energy transmitted having both direction and velocity is said to be a vector quantity. The magnitude of resultant (R), by vector analyses as shown in Figure- 3 a & b, can be determined with the help of Equation 5 and direction of resultant with respect to each coordinate axis viz., X-, Y- and Z-axis, can be determined with the help of Equations 6 a, b and c respectively. From the listed equations it is well understood that magnitude and direction of resultant will be governed by the component having the maximum magnitude i.e., the triggering component.

Table 1. P-wave velocity of different rock samples

| Material | P-wave velocity (m/s) | S-wave velocity (m/s) |
|------------------|-----------------------|-----------------------|
| Concrete | 3600 | 2000 |
| Granite | 5500-5900 | 2800-3000 |
| Basalt | 6400 | 3200 |
| Sandstone | 1400-4300 | 700-2800 |
| Limestone | 5900-6100 | 2800-3000 |
| Sand Unsaturated | 200-1000 | 80-400 |
| Sand Staurated | 800-2200 | 320-880 |
| Clay | 1000-2500 | 400-1000 |

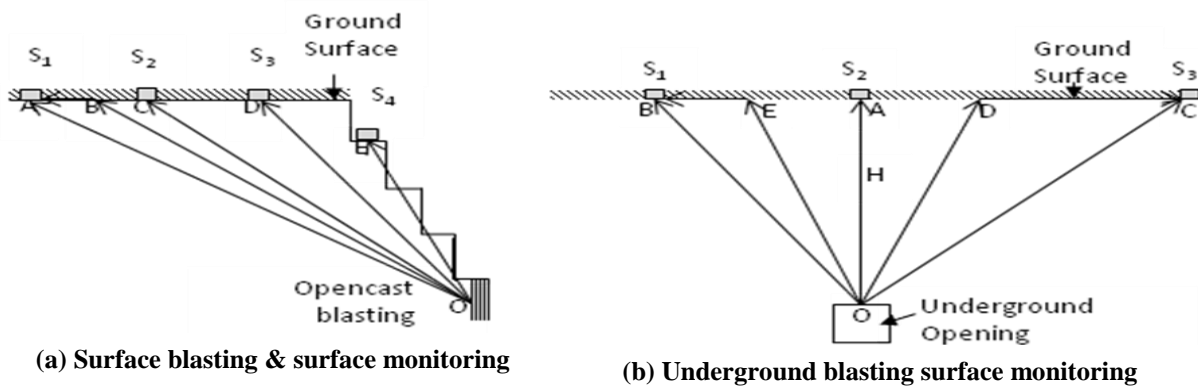


Figure 2. Typical wave transmission characteristics between blasts and monitoring points

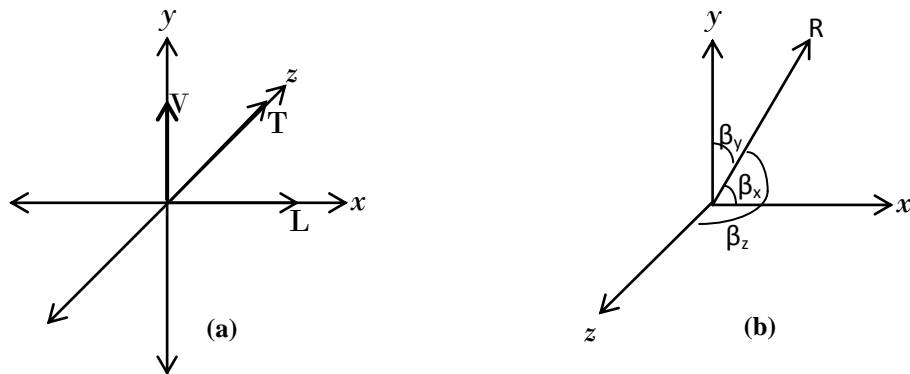


Figure 3. Vibrtrion velocity and resultant of three orthogonal components

$$R = \sqrt{V^2 + L^2 + T^2} \quad (5)$$

$$\text{Cos}(\beta_x) = \frac{L}{\sqrt{L^2 + V^2 + T^2}} \quad (6a)$$

$$\text{Cos}(\beta_y) = \frac{V}{\sqrt{L^2 + V^2 + T^2}} \quad (6b)$$

$$\text{Cos}(\beta_z) = \frac{T}{\sqrt{L^2 + V^2 + T^2}} \quad (6c)$$

4. Mathematical model

For proper fragmentation and heaving of blasted muck, blast geometry is limited by diameter and depth of blastholes. Application of wider blast geometry (Burden $\geq 0.4 \times$ Hole Depth) results into expansion of blasthole wall with up-heaving and minimum displacement of blasted muck. Fragmentation in such cases generally occurs by opening of joints during expansion of gas within blastholes with minimum catual breakage of rockmass. So, depending upon sensor location with respect to blast *i.e.*, elevation difference and horizontal distance, and the blast geometry implemented, variation in triggering component is observed.

Detonation of explosive generates maximum pressure in perpendicular direction to longer axis of blasthole *i.e.*, in 'P' direction, horizontal for vertical holes, and the magnitude decreases in other alternate paths *viz.*, 'P_i' at an angle γ with the major

stress direction Figure 4, Equation 7. However, with down-the-hole (NONEL) system of initiation, cooperation of blast waves from higher explosive column enhances velocity of blast wave along P_i direction, resulting into triggering of sensor by vertical component for longer distances of concern. So, will be the case for small diameter and shorter depth of blastholes. However, detonation of explosive from top *i.e.*, with fuse or detonating cord, longitudinal component may trigger the sensor at shorter distances. Interference of waves by less numbers of stratum vis-à-vis less attenuation in wave velocity result into such occurrence. Multi-layered transmission of blast waves results into absorption and refraction of waves vis-à-vis deterioration in intensity and velocity of blast wave. This results into increase in both travel distance and time to cause late arrival of body waves and an early arrival of combination of body and surface wave *viz.*, longitudinal component to trigger the sensor to monitor. For normal blast geometries *i.e.*, burden varying between 0.25-0.35 times the depth of blasthole, vertical component will trigger at closer distance and longitudinal component will trigger at greater distances. However, wider blast geometries or low charge consumption results into increased borehole pressure and high velocity of body waves to enable the sensors located at even longer distances to get triggered by either vertical or transverse component. Blast details and corresponding triggering component with respect to distance of measurement for some blasts in overburden benches of opencast mine is given in Table 2. For serial Nos. 1-3, vibration monitoring was carried out in the same bench. In these blasts it

Table 2. Blast details and vibration triggering component for different distances and type of blasts

| BLAST DETAILS | | | | | VIBRATION DETAILS | | | | | | |
|--|-------------------|--------------------------|----------------------|-------------------|-------------------|----------------------|-------------------|-----------------|---------------------|-------------------------------|----------------|
| Serial No. | Depth of hole (m) | Burden x Spacing (m x m) | System of Initiation | Total Charge (kg) | Distance (m) | Triggering Component | Transverse (mm/s) | Vertical (mm/s) | Longitudinal (mm/s) | Peak Particle Velocity (mm/s) | Frequency (Hz) |
| Mine A: (Kooreidih OCP, Block IV), BCCL | | | | | | | | | | | |
| 1 | 14 | 3.5 x 3.7 | NONEL | 1755 | 165 | Long | 1.52 | 1.65 | 2.67 | 3.12 | 7.2 |
| | | | | | 184 | Long | 1.84 | 1.71 | 1.59 | 2.40 | 8 |
| | | | | | 200 | Long | 0.889 | 1.78 | 2.1 | 2.30 | 7 |
| 2 | 7 | 3.5 x 3.7 | NONEL | 375 | 85 | Vert | 3.49 | 3.05 | 6.03 | 6.46 | 15 |
| | | | | | 100 | Long | 2.98 | 1.78 | 4.45 | 4.75 | 14 |
| | | | | | 140 | Vert | 1.27 | 1.14 | 1.27 | 1.55 | 12 |
| 3 | 6 | 3.5 x 3.7 | NONEL | 305 | 100 | Vert | 2.03 | 2.54 | 1.59 | 2.86 | 43 |
| | | | | | 145 | Long | 1.27 | 1.52 | 1.40 | 1.87 | 9.5 |
| | | | | | 170 | Vert | 0.699 | 1.27 | 0.572 | 1.33 | 6 |
| Mine B: Jamuna Kotma OCP, MCL | | | | | | | | | | | |
| 4 | 11.6 | 6.4 X 7.0 | NONEL | 5262.6 | 331 | Vert | 2.68 | 2.48 | 1.95 | 2.90 | 10 |
| | | | | | 366 | Vert | 2.68 | 2.48 | 1.95 | 2.49 | 7 |
| | | | | | 396 | Vert | 1.4 | 1.52 | 1.46 | 2.05 | 5.88 |
| | | | | | 432 | Vert | 1.06 | 1.54 | 1.44 | 1.73 | 5 |
| | | | | | 467 | Long | 0.762 | 1.14 | 1.14 | 1.38 | 5 |
| 5 | 11 | 6.4 x 7.0 | NONEL | 11024.6 | 350 | Vert | 1.83 | 1.79 | 1.83 | 2.43 | 5.5 |
| | | | | | 386 | Long | 1.65 | 1.08 | 1.40 | 1.76 | 5 |
| | | | | | 418 | Long | 1.08 | 1.46 | 1.52 | 1.62 | 5.5 |
| | | | | | 456 | Long | 1.17 | 1.03 | 1.30 | 1.61 | 5 |
| | | | | | 492 | Long | 0.635 | 0.762 | 1.02 | 1.03 | 15.5 |
| 6 | 2.8 | 2.8 x 3.1 | DETONATING CORD | 375 | 192 | Trans | 0.952 | 1.40 | 1.03 | 1.44 | 14 |
| | | | | | 242 | Long | 1.02 | 0.445 | 0.826 | 1.05 | 17 |
| | | | | | 215 | Vert | 1 | 1.87 | 3.65 | 4.05 | 7 |
| 7 | 2.5 | 2.5 x 2.8 | DET CORD | 500 | 245 | Vert | 1.52 | 2.25 | 3.46 | 4.01 | 5 |
| | | | | | 276 | Vert | 1.02 | 1.84 | 3.62 | 3.86 | 7 |
| | | | | | 307 | Long | 0.762 | 1.59 | 1.78 | 1.94 | 7 |
| | | | | | 337 | Vert | 0.762 | 1.27 | 1.65 | 1.71 | 9 |

was observed that for longer depth of blastholes (14 m), sensor got triggered by longitudinal component only. However, for shorter depth of blast holes (6-7 m), sensor located nearest and farthest to blast locations got triggered by vertical component and intermediate distance by longitudinal component. Similarly, Blast nos. 4 and 5 of Table 2 monitoring of vibration was carried out with a maximum elevation difference of about 25 m, where the sensor was located above the blast locations. However, for shorter depth of blasts, blast nos. 6 & 7 having no free face had an elevation difference of about 45-50 m. Comparative analyses of vibration records for blast nos. 4 & 5 indicates that increased total charge resulted into longitudinal component triggering the sensor at closer distances. However, measurements at greater elevation difference (blast nos. 6 & 7), but, with detonating cord system resulted into

longitudinal component triggering the sensor even at closer distances. Similar is the case for the blast information detailed in Table 3. In Table 3, it is observed that for 11 m depth of holes, longitudinal component triggered the sensor for the two measurements made at more than 1200 m from the blast. However, for shorter depth of blastholes (≈ 6 m), but, same type of initiation system (NONEL), the triggering component (vertical/transverse and longitudinal) varied with distance of measurement. For Blast No. 3, Table 3, vertical component triggered the sensor located at 1392 and 1480 m and on contrary, in Blast No. 6, Table 3, it is observed that longitudinal component triggered the sensor at 1405 m and 1552 m, indicating the influence of initiation system on triggering component.

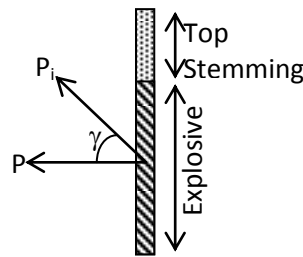


Figure 4. Schematic diagram showing stress wave direction with detonation of explosive

$$P_i = PCos(\gamma) \quad (7)$$

For underground blasting and surface monitoring, the component triggering the sensor to monitor would depend upon location of sensor with respect to vibration source and P-wave velocity of transmitting medium. For most of the underground blasts and surface monitoring, vertical or transverse component indicates maximum magnitude and triggers the sensor to monitor. However, when instrument is located at greater horizontal distance in comparison to vertical cover or in presence of void (underground workings or worked out area) between blast and instrument location, longitudinal component will trigger the sensor to monitor. Blast nos. 7 and 8 in Table 3 represents surface monitoring for underground blasts. Here it is observed that at intermediate distance longitudinal component triggered the sensor and for rest of the locations, the sensor got triggered by either vertical or transverse component.

5. The model

Triggering component for any sensor to monitor depends upon blast geometry, radial distance, 'Z', P-wave velocity of blast wave and absorption characteristics of different layers within transmitting medium (Figure 5). Horizontal and elevation difference between vibration source and sensor be represented by 'X' and 'Y' respectively. Here, 'A' is the location of sensor and 'C' is source of vibration. Using Pythagoras theorem, radial distance 'Z' can be determined by Equation 8 and using simple trigonometric functions, Equation 8 can be reduced to Equations 9 and 10, each independent of 'Y' and 'X' respectively, but with an additional parameter viz., the refracted angle 'θ' within the stratum.

Table 3. Blast details and vibration triggering component for different distances and type of blasts

| BLAST DETAILS | | | | | VIBRATION DETAILS | | | | | | |
|--|-------------------|--------------------------|----------------------|-------------------|-------------------|----------------------|-------------------|-----------------|---------------------|-------------------------------|----------------|
| Serial No. | Depth of hole (m) | Burden x Spacing (m x m) | System of Initiation | Total Charge (kg) | Distance (m) | Triggering Component | Transverse (mm/s) | Vertical (mm/s) | Longitudinal (mm/s) | Peak Particle Velocity (mm/s) | Frequency (Hz) |
| Mine C: Samleshwari OCP, MCL | | | | | | | | | | | |
| 1 | 11 | 3.5 X 4.5 | NONEL | 4860 | 1245 | Long | 0.762 | 0.381 | 1.14 | 1.26 | 10 |
| | | | | | 1808 | Long | 0.889 | 0.445 | 0.587 | 1.02 | 8 |
| | | | | | 541 | Long | 5.33 | 3.17 | 6.10 | 6.16 | 7.9 |
| 2 | 6 | 4 X 4 | DETONATING CORD | 5840 | 648 | Long | 4.83 | 3.37 | 5.40 | 5.94 | 19 |
| | | | | | 680 | Trans | 2.83 | 2.37 | 2.98 | 3.24 | 20 |
| | | | | | 717 | Vert | 3.11 | 1.84 | 3.81 | 3.87 | 16 |
| 3 | 6.0 | 4 X 4 | NONEL | 4930 | 1392 | Vert | 1.40 | 0.762 | 0.889 | 1.44 | 11 |
| | | | | | 1440 | Long | 1.21 | 0.508 | 0.889 | 1.35 | 16 |
| | | | | | 1480 | Vert | 1.10 | 0.762 | 0.937 | 1.14 | 10 |
| 4 | 6.0 | 4 X 4 | DETONATING CORD | 4970 | 432 | Long | 4.83 | 2.41 | 4.57 | 5.87 | 11 |
| | | | | | 464 | Vert | 2.48 | 1.97 | 3.56 | 4.59 | 24 |
| | | | | | 504 | Vert | 3.87 | 2.22 | 3.43 | 4.49 | 18 |
| 5 | 6.0 | 4 X 4 | NONEL | 3150 | 544 | Vert | 3.41 | 2.13 | 3.92 | 4.35 | 10 |
| | | | | | 1405 | Long | 0.762 | 0.762 | 1.14 | 1.21 | 18 |
| | | | | | 1456 | Trans | 0.508 | 0.191 | 0.381 | 0.524 | 15 |
| | | | | | 1552 | Long | 0.302 | 0.302 | 0.317 | 0.397 | 15 |
| Mine D: Bartarai Underground Coal Mine, MCL | | | | | | | | | | | |
| 6 | | | Detonator | 7.77 | 88.85 | Trans | 1.21 | 0.381 | 0.572 | 1.37 | 64 |
| | | | | | 95.78 | Vert | 0.381 | 0.889 | 0.381 | 0.905 | 73 |
| | | | | | 98.46 | Long | 0.476 | 0.413 | 0.762 | 0.902 | 39 |
| | | | | | 93.32 | Trans | 0.826 | 0.317 | 0.381 | 0.921 | 64 |
| 7 | | | Detonator | 7.77 | 94.12 | Vert | 0.540 | 0.825 | 0.619 | 0.884 | 57 |
| | | | | | 99.12 | Long | 0.492 | 0.397 | 0.794 | 0.826 | 47 |
| | | | | | 108.85 | Vert | 0.381 | 0.762 | 0.381 | 0.810 | 64 |
| | | | | | 111.36 | Vert | 0.381 | 0.699 | 0.381 | 0.699 | 64 |

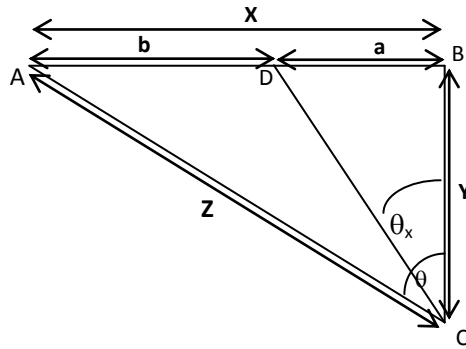


Figure 5. Schematic diagram showing sensor location, A, with respect to blast location, C

$$Z^2 = X^2 + Y^2 \quad (8)$$

$$Z^2 = X^2 \text{Cosec}^2(\theta) \quad (9)$$

$$Z^2 = Y^2 \text{Sec}^2(\theta) \quad (10)$$

From the above diagram it is well understood that propagation of blast wave to trigger the sensor will travel through either path ‘CA’ or along a variable path ‘CD and DA’. From trigonometric equations, magnitude of the variable path ‘CD’ can be determined from Equation 11. The above equation clearly indicates that with an increasing value of ‘ θ_x ’, the travel distance and time for wave propagation along path CD increases. Velocity of S-wave (V_s) being about 60% of P-wave (V_p) velocity, body wave will trigger the sensor to monitor till travel time along the hypotenuse is less than the other alternate paths. However, in jointed or stratified stratum, velocity of body wave decreases due to absorption, refraction and internal reflection within the filling material. So, increased travel distance and depleting wave propagation velocity when transmitted through different layers along path CA may result into an early arrival along the arbitrary path along CD and DA. This will result into triggering of sensor by surface wave *i.e.*, longitudinal component. Equating the inequalities of travel time along path ‘CA’ and along path ‘CD and DA’, the triggering component will vary and is represented by Equations 12 and 13 respectively.

$$CD = \frac{2a \sin \theta_x \pm \sqrt{4a^2 \sin^2 \theta_x - 4(a^2 - Y^2)}}{2} \quad (11)$$

Vertical or transverse component will trigger the sensor to monitor, if

$$\frac{CD}{V_b} + \frac{b}{0.6V_b} \geq \frac{\sqrt{Y^2 + (a+b)^2}}{V_b} \quad (12)$$

Similarly, longitudinal component will trigger the sensor to monitor, if

$$\frac{CD}{V_b} + \frac{b}{0.6V_b} \leq \frac{\sqrt{Y^2 + (a+b)^2}}{V_b} \quad (13)$$

For stratified strata, travel distance of blast wave within a stratum and its attenuation would vary with rock mass properties, wave velocity and absorption characteristics of each stratum. For an incident angle ‘ ϕ_i ’ and thickness ‘ Y_i ’, of a stratum, the travel distance within that strata ‘ Z_i ’ will vary with angle of refraction ‘ ϕ_r ’. Travel time will similarly vary with characteristics of absorption within the strata and can be evaluated by using Equations 1-4. Considering ‘N’ number of strata in the path of travel, actual travel time to the sensor location can be determined by cumulative summation of travel time in each stratum. Travel time or distance of travel in each stratum can be determined with the help of Equations 14-16. Thereafter, summation of travel times in each stratum will result into actual travel time of body wave by using Equation 17. However, surfaces of each strata being not smooth, angle of refracted wave will vary to cause an early reach of body wave to surface and thereafter reach the sensor to trigger as surface wave. Evaluation of travel time of body wave for each degree within the solid angle created by vertically above the blast, detonation locus and the sensor location (here angle BCA, Figure-5) and consecutive summation of simulated travel time of surface wave for the length upto the sensor after reaching of body wave to the surface can be made. Comparison between two types of wave transmission *viz.*, only body wave and combination of body and surface wave, characteristics of blast wave (body or combination of body and surface wave) that will trigger the sensor will vary.

$$f(a) = Z_i \frac{\partial z}{\partial t} = X_i \frac{\partial x}{\partial t} + Y_i \frac{\partial y}{\partial t} \quad (14)$$

$$f(b) = Z_i \frac{\partial z}{\partial t} = X_i \text{Co sec}^2(\phi_i) \frac{\partial x}{\partial t} \quad (15)$$

$$f(c) = Z_i \frac{\partial z}{\partial t} = Y_i \text{Sec}^2(\phi_i) \frac{\partial y}{\partial t} \quad (16)$$

$$\text{Traveltime}(s) = \sum_1^N [f(a)] \text{or} [f(b)] \text{or} [f(c)] \quad (17)$$

6. Structural analyses

Masonry wall structures are either load bearing or non-load bearing type. The brick and mortar constructed structures of mining area generally possess load bearing walls. Masonry structures, having two material qualities *viz.*, stiffer (brick) and relatively softer (mortar), may grow cracks due to moisture absorption or thermal expansion of bricks which results into either shrinkage in concrete masonry unit or expansion in brick masonry unit. Comparative study of strain produced due to blasting (dynamic) and environmental changes (static) illustrate that the static changes are more prone to damage than that caused by blasting [19]. Compressive strength of bricks, though, varies between 2 and 24 MPa, flexural strength and durability of structure depends upon initial rate of water absorption and absorption capacity by bricks [20-22]. Stiffness of structure *vis-à-vis* structural height with respect to thickness of wall influences cohesive binding force between brick components because structures are less stable against lateral load *i.e.*, they are very weak in tension. Flexural strength of brick and mortar construction varies between 0.1 and 0.414 MPa and bond strength between 0.054 and 0.265 MPa. Blast loads typically produce strain rate in the range between 102 and 104 s⁻¹; much lower than dynamic failure loading strain for brick and mortar constructed structures [23, 24].

Structures located in proximity to blast sites (elastic zone) are regularly excited to oscillate. Sustainability of any structure without getting damage depends upon magnitude of excitation along each component, dimension of structure with respect to source of vibration and phase difference between the components causing excitation, Figure 6. The Figure clearly states that structures with greater dimension against the blast *i.e.*, X-Y plane, will suffer more damage than a structure with lesser dimension facing the blast *i.e.*, along Y-Z or Z-X

plane. Variation in moment of inertia along each direction results into difference in stress developed on walls (Equations 18 and 19) and hence, sustainability towards vibration magnitude. Moment of inertia for three-dimensional body is obtained by adding its moment with respect to the axis passing through the centroid and thereafter transformed into any required parallel axis as product of the mass of the body and square of the distance between the two axes (Equation 20). But, presence of rigidly well connected structured frames, sometimes increases sustainability by restoring differential stress within the structure and results into minimum wall deflection *vis-à-vis* bending stress on each wall (Figure 7 a and b). However, difference in excitation of two opposite walls without any well connected frames might result into difference in amplitude of wall oscillations. The stress developed due to differential deflection of opposite walls when exceeds the cohesive binding strength between brick and mortar might result into cosmetic cracks on plaster wall or in mortar placed between bricks. So, depending upon the cohesive binding strength of mortar and the stress developed due to bending cracks will develop along hade joints or bed joints. Analyses of structural safety due to bending (deflection), in three orthogonal directions, it is well understood that in comparison to vertical or transverse components, longitudinal component is more susceptible to cause damage to structure. Action of longitudinal component along bed joints, weakest amongst the brick and mortar structure, results into weakening of these joints to develop cosmetic cracks in plaster. However, transmission of vertical component *i.e.*, in perpendicular direction to bed joint, results into compression of brick and mortar to cause minimum damage to structure. Similarly, minimum damage to structure will also occur by transverse vibration component as it acts perpendicular to hade joint and in longer axis of bed joint.

$$I_x = \frac{W}{g} \frac{H^2 + B^2}{12}; I_y = \frac{W}{g} \frac{L^2 + B^2}{12}; \quad (18)$$

$$I_z = \frac{W}{g} \frac{L^2 + H^2}{12}$$

$$\frac{M}{I} = \frac{f}{y} = \frac{E}{R} \quad (19)$$

$$i^2 = \bar{i}^2 + d^2 \quad (20)$$

Where,

i = moment of inertia of three-dimensional body about the axis

\bar{i} = moment of inertia of two-dimensional body about that axis,

d = distance of centroid along that axis,

M = Bending moment along neutral axis,

y = distance from the centroidal axis,

E = Young's Modulus,

f = stress developed due to bending,

I = Moment of Inertia,

R = Radius of curvature,

W = Weight of structure, and

g = acceleration due to gravity.

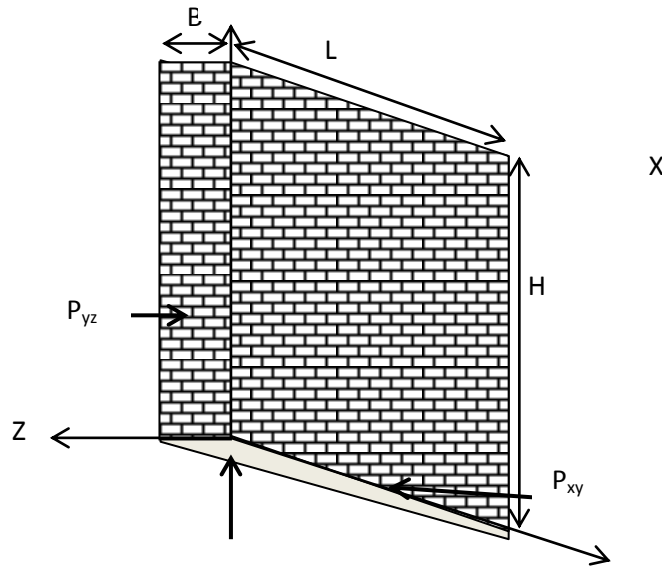
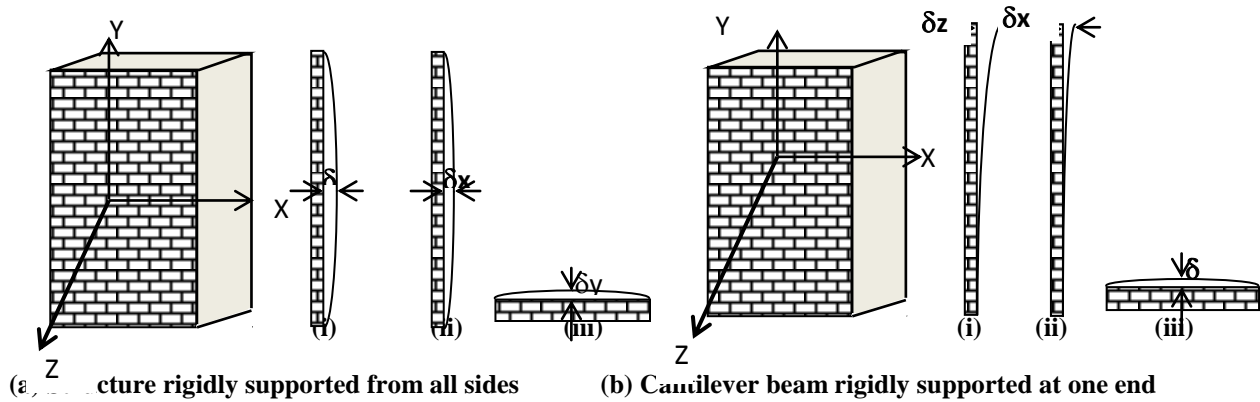


Figure 6. Brick and mortar constructed wall under various vibration components



Force along (i) X-Y Plane; (ii) Y-Z Plane; (iii) Z-X Plane

Figure 7. Types of deflection of rigidly and cantilevered supported wall

7. Conclusions

Mechanism of rock breakage and rockmass properties of individual stratum principally governs the component that will trigger the sensor to monitor. Characteristics of reaction force vis-à-vis borehole pressure and the distance of monitoring determines the component that will trigger the sensor to monitor. For normal blast geometry, vertical component of blast wave will trigger the sensor at closer distances and longitudinal component will trigger the sensor located at far off distances. But, when magnitude of burden is high in comparison to diameter and depth of blastholes, rock breaks principally by crater mechanism. High borehole pressure results into vertical component to trigger the sensor even for longer distances of concern. This may also be observed when elevation difference between blast source and location of monitoring is very high. However, more monitoring is to be carried out for justification of the model. Considering moment of inertia for three orthogonal directions, vertical or transverse component of vibration generates least bending stress vis-à-vis damage to structures. So, in addition to magnitude of peak particle velocity, particle velocity in three orthogonal directions should be considered to evaluate safety of structures.

References

- [1]. Sisking, D. E., Stagg, M. S., Kopp, J. W. and Dowding, C. H. USBM report of Investigation 8507. Structure response and damage produced by ground vibration from surface mine blasting.
- [2]. German Institute of Standards. (1986). Vibration of building-effects on structures. DIN 4150, Vol. 3. 1-5.
- [3]. DGMS (Tech) S.&T Circular No. 7. (1997). Damage of the Structures due to blast induced ground vibration in the mining areas.
- [4]. Chae, Y. S. (1978). Design of excavation blasts to prevent damage. Civil Engineering, ACSE. 48 (1): 77-79.
- [5]. Bay, J. A. (2003). A summary of the research on pile driving vibrations, Proc. Of 7th Pile Driving Contractors Association Annual Winter Roundtable, Atlanta, GA.
- [6]. Siskind, D. E. and Stagg, M. S. USBM Report of Investigation 8969. Blast vibration measurements near and on structure foundations.
- [7]. Svinkin, M. R., Shaw, A. G. and Williams, D. (2000). Vibration environment effect of construction operations. DFI 25th Annual Meeting and Eighth Int. Conf. and Exhibition, A Global prespective on Urban Deep Foundations, New York. 483-491.
- [8]. Svinkin, M. R. (2002). Predicting soil and structure vibrations from impact machines. Jr. of Geotechnical and GeoEnvironmental Engg. 138 (7): 602-612.
- [9]. Mandal, S. K., Singh M. M. and Dasgupta, S. (2005). A theoretical concept of structural dynamics to evaluate blast-induced damage on structures. Mining Technology (Trans. Inst. Min. Metall. A) Vol. 114. 219-226.
- [10]. Mandal, S. K. (2010). Blast wave characteristics and its influence with distance of measurement, International Journal of Mining and Mineral Engineering, Inderscience Publishers. 2 (1): 30-43.
- [11]. Fournay, W. L., Barker, D. B. and Holloway, D. C. (1983). Fragmentation in jointed rock material, Proc. of 1st Int. Symp. on Rock fragmentation by blasting, Lulea, Sweden, Vol. 2. 505-531.
- [12]. Fournay, W. L., Dick, R. D., and Wang, X. J. and Wei, J. (1993). Fragmentation mechanism in crater blasting, Int. JI. Of Rock Mech., Min. Science and Geomech. Abs. 30 (4): 413-429.
- [13]. Simha, K. R. Y. (1993). Stress wave patterns in tailor pulse loading, Proc. IV Int. Symp. On Rock Fragmentation by Blasting-FRAGBLAST -4, Vienna, Austria ed. H. P. Rossmannith. 79-85.
- [14]. Simha, K. R. Y. (1996). Effect of open joint on stress wave propagation. Proc. Of the 5th Int. Symp. On Rock Frag. By Blasting, (ed. Mohanty), Montreal, Canada. 81-86.
- [15]. Blair, D. P. (2004). Charge weight scaling laws and the superposition of blast vibration waves. J. on Rock Fragmentation by Blasting, FRAGBLAST. 8 (4): 221-239.
- [16]. Guo, Z. Q. (1982). "Wave in Solid Objects," Earthquake Publishing House, Beijing.
- [17]. Kolsky, H. (1983). "Stress Waves in Solids," Dover Publications Inc., New York.
- [18]. Mandal, S. K. Singh, M. M. and Bhagat, N. K. (2013). Particle Velocity of Ground Vibration Reflects Mechanism of Rock Breakage and Damage to Structures. Journal of Civil Engineering Services. 2 (1): 178-183.
- [19]. Dowding, C.H. (1996). "Construction Vibrations" Prentice Hall, Upper Saddle River.
- [20]. Sarangapani, G., Venkatarama Reddy B. V. and Jagadish, K. S. (2002). Stuctural characteristics of bricks, mortars and masonry. J. of Structural Engg. 29 (2): 101-107.

[21]. Parashar A. K. and Parashar, R. (2012). Comparative Study of Compressive Strength of Bricks Made With Various Materials to Clay Bricks. *International Journal of Scientific and Research Publications*. 2 (7): 1-4.

[22]. Drysdale, R. G., Hamid, A. A., and Baker, L. R. (1994). *Masonry structures: Behaviour and design*, Prentice-Hall, Englewood Cliffs, N.J.

[23]. Grote, D.L., S.W. Park and M. Zhou. (2001). Dynamic behavior of concrete at high strain rates and pressures: Experimental characterization. *Inter. J. Impact Eng.* 25: 869-886.

[24]. Taher Abu-Lebdeh, Sameer Hamoush, Wonchang Choi and Moayyad Al Nasra. (2011). High Rate-Dependent Interaction Diagrams for Reinforced Concrete Columns, *American J. of Engineering and Applied Sciences*. 4 (1): 1-9.